Supporting Information

Growth of Macroporous TiO_2 on B doped g-C_3N_4 Nanosheet: A Z-Scheme Photocatalystfor H_2O_2 Production and Phenol Oxidation under Visible Light

Arjun Behera, Pradeepta Babu, and Kulamani Parida*

Centre for Nanoscience and Nanotechnology, Siksha 'O' Anusandhan, Bhubaneswar 751030, India

Table S1: Literature survey on various TiO_2/g-C_3N_4 systems

Photocatalyst	Synthesis method	Activity	Reference
TiO_2/C_3N_4	Hydrothermal	H_2 and O_2 generation of 50.2 and 24.3μmol/ h	1
TiO_2/C_3N_4	Mechanical mixing	57 % N_2O conversion in 16h	2
TiO_2–C_3N_4	Hydrothermal	94.6 % RhB degradation in 60 min	3
C/X-TiO_2@C_3N_4 (X = N, F, Cl)	Sol-gel-pyrolysis	74.7% p-chlorophenol degradation in 6h	4
N,S-TiO_2/g-C_3N_4	Thermal process	125 μmol/h H_2 evolution	5
TiO_2/B doped g-C_3N_4	Sonication followed by calcination methods	87% of 20 ppm phenol in 2h, H_2O_2 production 22 μmol/h	Present work

Table S2: Crystallite size of different photocatalyst based on Williamson- Hull and Scherer method.

Photocatalyst	Crystallite size (D) (nm) W-H analysis	Crystallite size (D) (nm) Scherer analysis
P25	**28.81**	**28.74**
TiO_2	**57.27**	**59.16**
E-BCN	**1.38**	**2.1**
TBCN-4	**24.31**	**23.24**
TBCN-8	**69.30**	**64.97**
TBCN-12	**49.5**	**48.41**

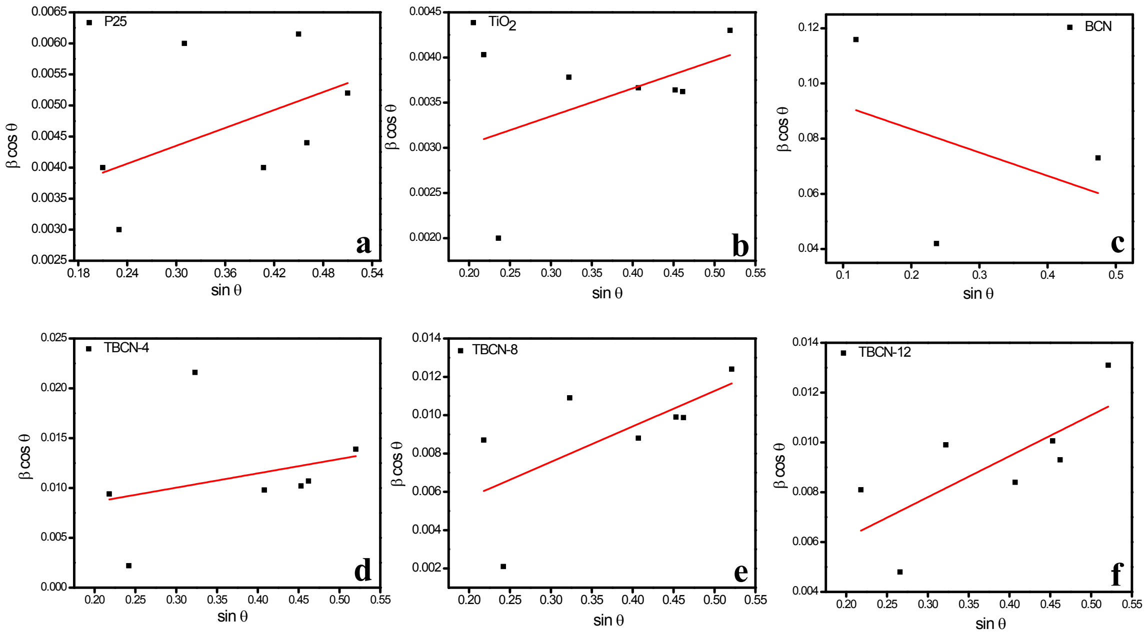

Figure S1: W-H plot of different photocatalyst.

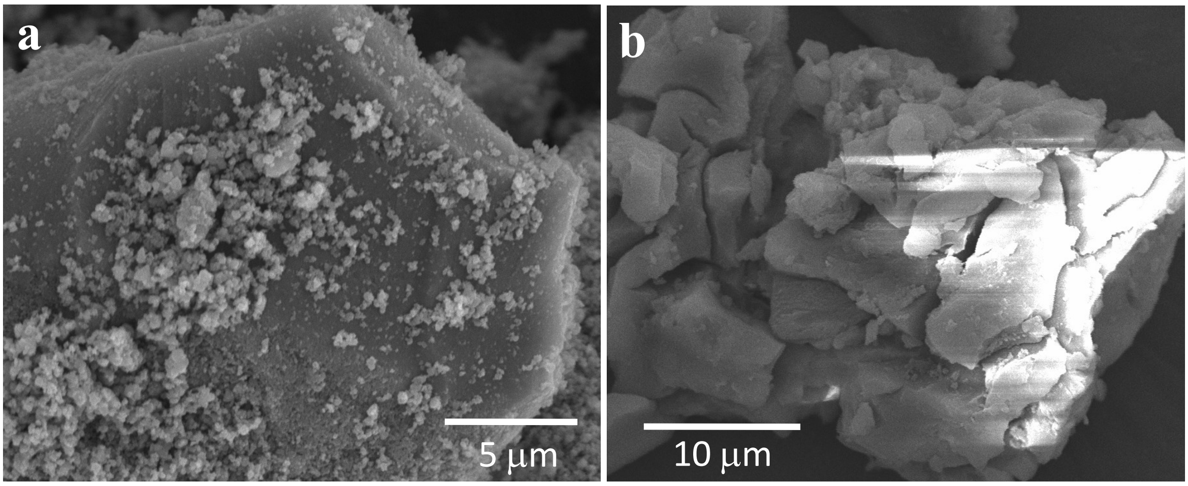

Figure S2: SEM images of neat TiO_2 and BCN.

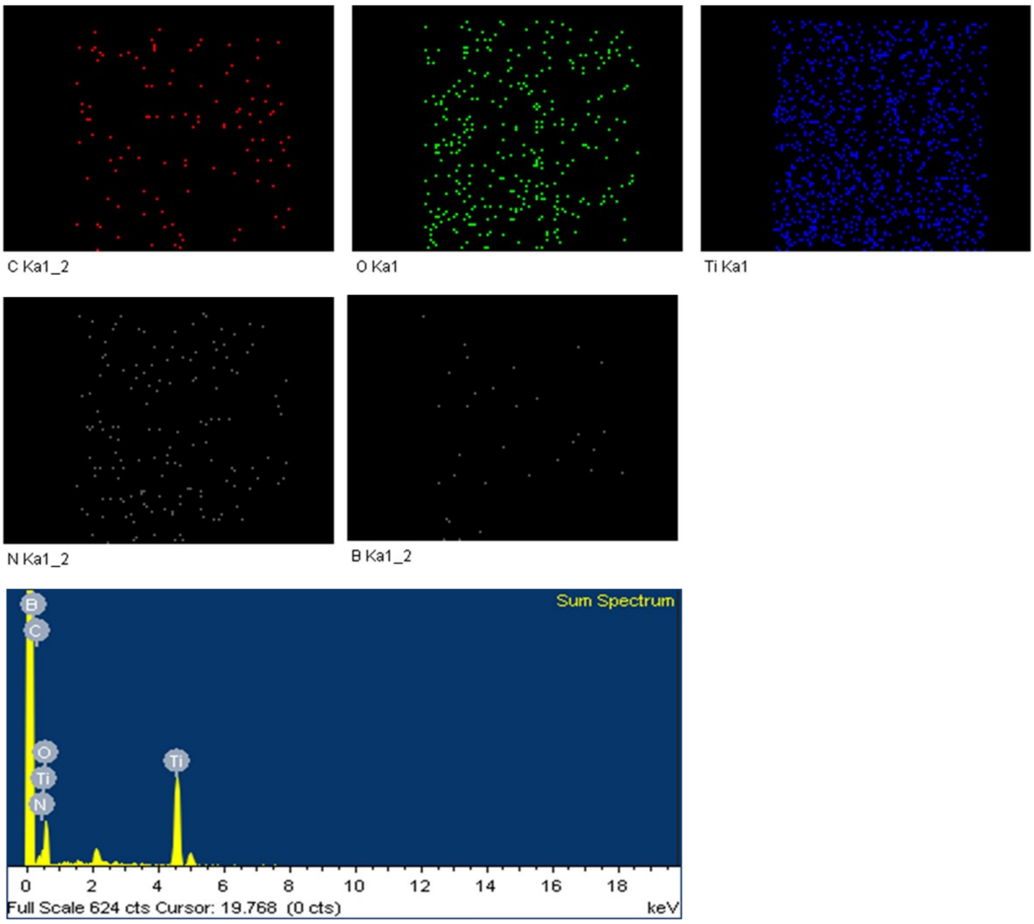

Figure S3: Elemental mapping and EDX spectra of TBCN nanocomposites.

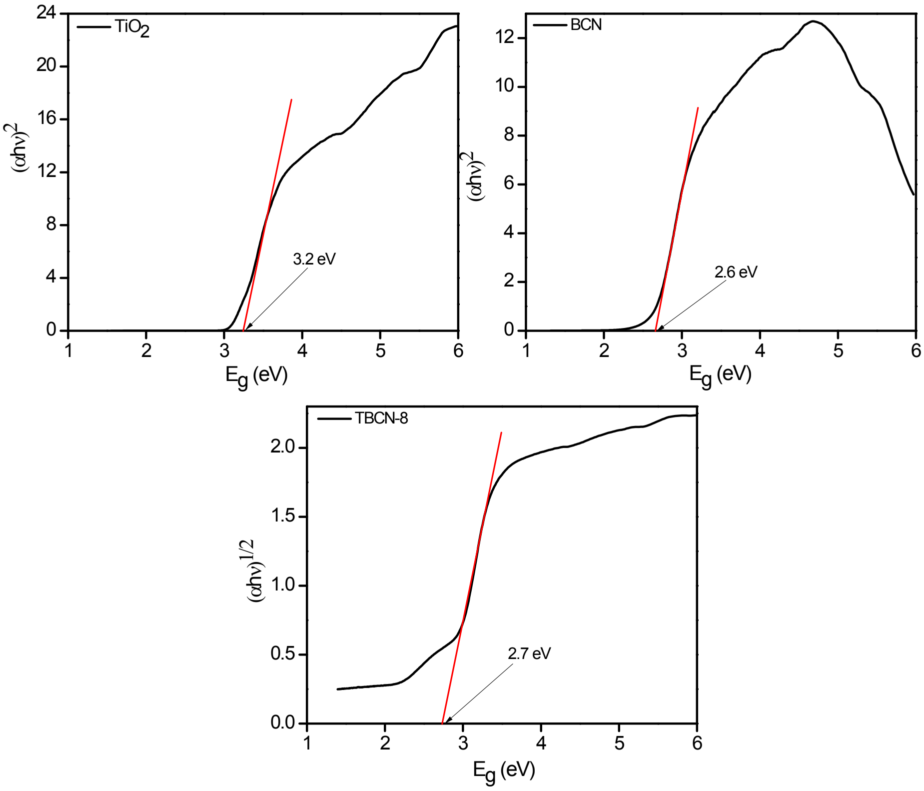

Figure S4: (a, b) Direct band gap plot of BCN and pure TiO_2 (c) Indirect band gap plot of TBCN-8 nanocomposites.

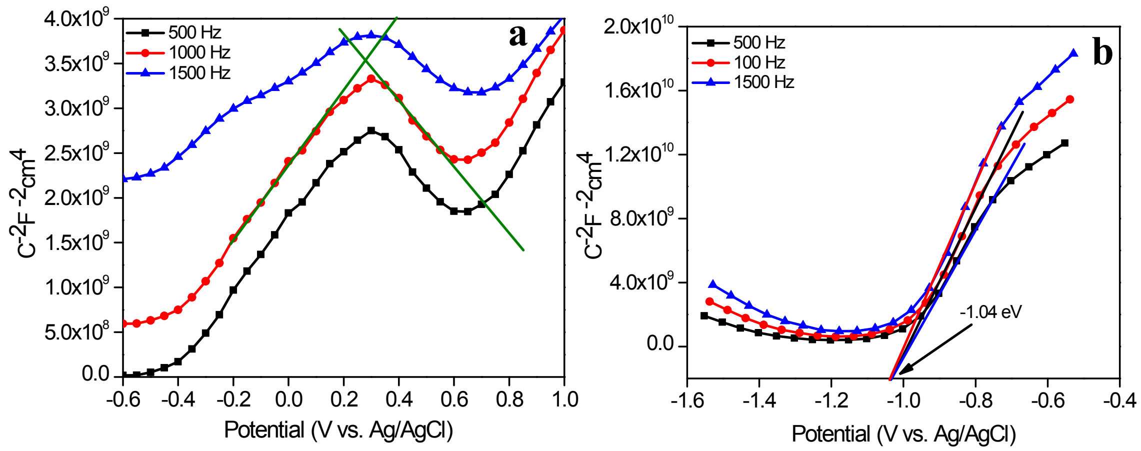

Figure S5: (a) Mott-Schkotty plot of TBCN-8 composites (b) MS plot of TiO_2 with different frequencies (500, 1000 and 1500 Hz).

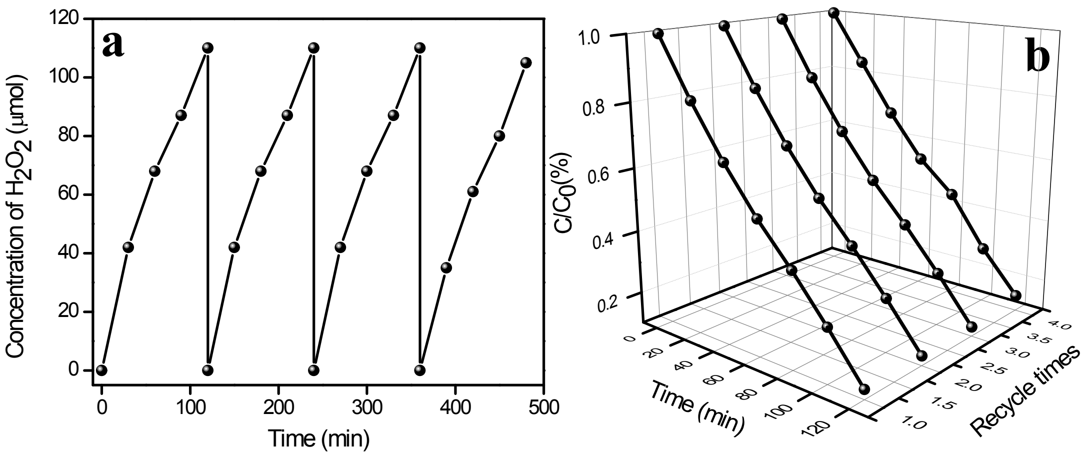

Figure S6: (a) Stability plot of H_2O_2 concentration for consecutive four cycle (b) Reusability plot of phenol oxidation up to 4 cycles.

Table S3: 1st order kinetics results of phenol over as synthesized photocatalyst.

Catalysts	R^2	k_{obs} **(min**$^{-1}$**)**	$t_{1/2}$ **(min)**	**% of phenol oxidation**
TiO_2	0.86	$7.4*10^{-3}$	93.6	62
BCN	0.93	$8.4*10^{-3}$	82.5	65
TBCN-4	0.94	$9.4*10^{-3}$	73.7	70
TBCN-8	0.92	$15.7*10^{-3}$	44.1	87
TBCN-12	0.95	$10.9*10^{-3}$	63.5	75

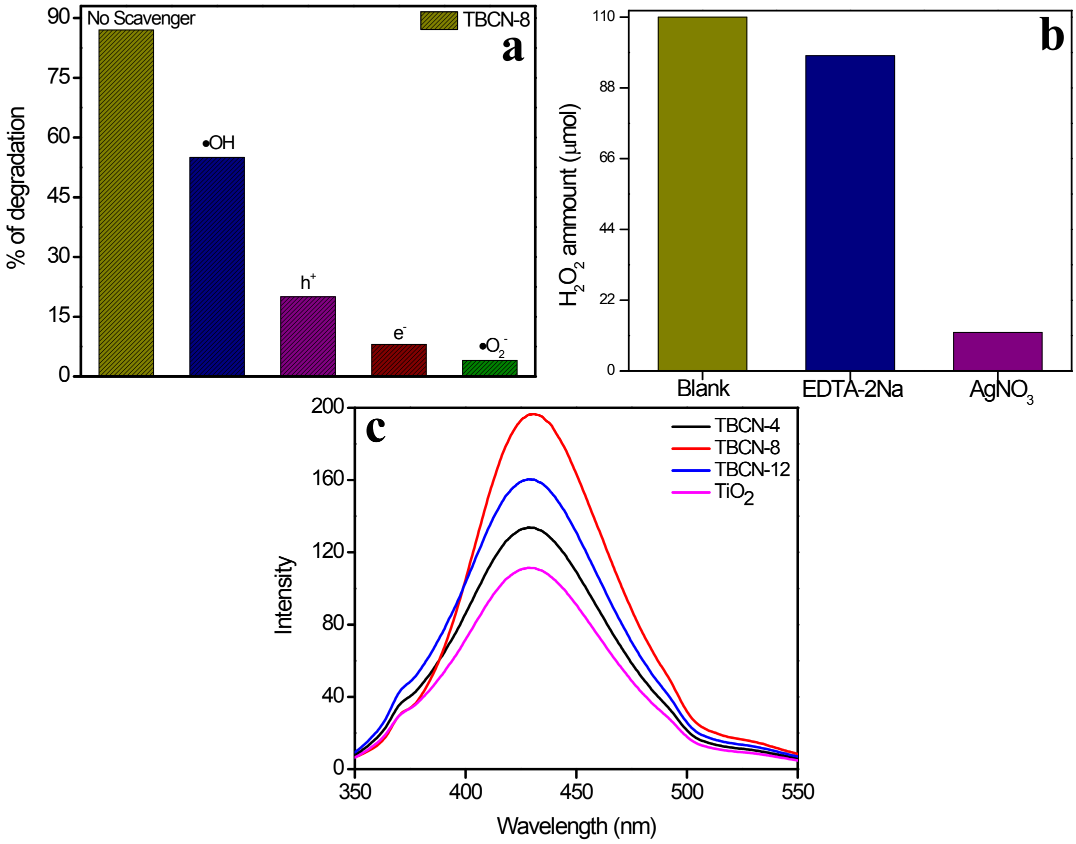

Figure S7: (a) Rate of phenol oxidation in the presence of different active species, which is responsible for photocatalytic degradation, processes (b) Scavenger test for photocatalytic H_2O_2 generation (c) Terepthalic acid tests for the generation of •OH radicals.

Reference

(1) J. Yan, H. Wu, H. Chen, Y. Zhang, F. Zhang, S. F. Liu, Fabrication of TiO_2/C_3N_4 heterostructure for enhanced photocatalytic Z-scheme overall water splitting. *Appl. Catal. B: Envirol.*, 2016, **191**, 130-137.

(2) M. Reli, P. Huo, M. Šihor, N. Ambrozova, I. Troppová, L. Matejova, P. Praus, Novel TiO_2/C_3N_4 photocatalysts for photocatalytic reduction of CO_2 and for photocatalytic decomposition of N_2O. *J Phys Chem A*, 2016, **120**, 8564-8573.

(3) W. Wang, Y. Liu, J. Qu, Y. Chen, M. O. Tadé, Z. Shao, Synthesis of hierarchical TiO_2–C_3N_4 hybrid microspheres with enhanced photocatalytic and photovoltaic activities by maximizing the synergistic effect. *ChemPhotoChem*, 2017, 1, 35-45.

(4) K. Li, Z. Zeng, L. Yan, M. Huo, Y. Guo, S. Luo, X. Luo, Fabrication of C/X-TiO2@ C3N4 NTs (X= N, F, Cl) composites by using phenolic organic pollutants as raw materials

and their visible-light photocatalytic performance in different photocatalytic systems. *Appl. Catal. B: Envirol.*, 2016*,* **187**, 269-280.
(5) S. Pany, K. M. Parida, A facile in situ approach to fabricate N, S-TiO_2/g-C_3N_4 nanocomposite with excellent activity for visible light induced water splitting for hydrogen evolution. *Phys. Chem. Chem. Phys.*, 2015, **17**, 8070-8077.